

# Electronic Structure and Mott Localization in Iron Deficient $\text{TlFe}_{2-x}\text{Se}_2$ with Superstructures

Chao Cao<sup>1</sup> and Jianhui Dai<sup>1,2</sup>

<sup>1</sup>Condensed Matter Physics Group, Department of Physics,  
Hangzhou Normal University, Hangzhou 310036, China

<sup>2</sup>Department of Physics, Zhejiang University, Hangzhou 310027, China  
(Dated: December 2, 2024)

Electronic structure and magnetic properties for iron deficient  $\text{TlFe}_{2-x}\text{Se}_2$  compounds are studied by first-principles calculations. We find that for the case of  $x = 0.5$  with a Fe-vacancy ordered orthorhombic superstructure, the ground state exhibits a stripe-like antiferromagnetic ordering and opens a band gap only if the short-ranged Coulomb interaction of Fe-3d electrons is moderately strong, manifesting a Mott insulating state. While increasing Fe-vacancies from the  $x = 0$  side, where the band structure is similar to that of a heavily electron-doped FeSe system, the Mott localization can be driven by kinetic energy reduction as evidenced by the band narrowing effect. We also predict that for  $x = 0.5$  the Mott delocalization could take place under pressure up to  $\sim 6$  GPa.

PACS numbers:

The discovery of superconductivity (SC) with critical temperatures up to 56 K in iron pnictides [1–6] has triggered renewed interest in searching new route to high-temperature SC. Considerable concerns have been focused on the nature of the parent compounds which show variable bad metal behavior[7] and a universal strip-like antiferromagnetic (SDW) order[8]. The magnetic ordering was proposed to be the consequence of the low energy states ( or itinerant electrons ) within the nearly nested Fermi surfaces, and hence the Fermi surface nesting is responsible to SC when the SDW order is suppressed [9–11]. An alternative possibility is that the magnetic structure is due to the strong correlation among the Fe-3d electrons, so that the states far away from the Fermi surfaces should be taken into account as well. To this end, Fermi surface nesting is not a necessary ingredient and the  $J_1$ - $J_2$  Heisenberg model based on the local moment picture could be an appropriate starting point. [12–16]

Most recently, Fang *et al.* [17] reported that the Fe-deficient compounds  $(\text{Tl,K})\text{Fe}_{2-x}\text{Se}_2$  exhibit SC with  $T_c$  up to  $\sim 31$  K for  $x = 0.12 \sim 0.3$ . Special interests in this class of materials is that the SC emerges in proximity to an insulating phase. It is yet unknown whether this insulating phase is a Mott insulator driven by Fe-3d electron correlations. Theoretically, this possibility is mysterious, as the previously first-principle calculations on both  $\text{TlFe}_2\text{Se}_2$  [18] and  $\text{KFe}_2\text{Se}_2$  [19, 20] with the  $\text{ThCr}_2\text{Si}_2$  structure (122-type) suggest that the parent compounds of the ternary iron chalcogenides should be metallic with either checkboard antiferromagnetic (AFM) (for Tl-122)[18] or SDW (for K-122)[20] order, much like the electron overdoped 11-type iron selenides. Experimentally, it has been reported recently that the alkali intercalated compounds  $\text{K}_{0.8}\text{Fe}_2\text{Se}_2$ [21] and  $\text{Cs}_{0.8}\text{Fe}_2\text{Se}_{1.96}$  [22] ( both iso-structural to  $\text{BaFe}_2\text{As}_2$ ), while superconducting under 30 K and 27 K respectively, exhibit the metallic behavior in their normal states.

Two closely related questions thus arise: What is the ground state of the "parent" compound of these superconducting ternary iron chalcogenides of 122-type structure, and how can a Mott-insulating phase develop and then diminish with in-

creasing Fe-content or *electron doping* giving rise to SC?

In this paper, we suggest partial answers to the questions by first-principles study on  $\text{TlFe}_{2-x}\text{Se}_2$ . We start from and pay special attention to the case with  $x = 0.5$ , which is stoichiometrically equivalent to  $\text{Tl}_2\text{Fe}_3\text{Se}_4$  but with Fe vacancies in the 122-type structure. Hence,  $\text{Fe}^{2+}$  is the nominal valence as in other iron pnictides/chalcogenides. Our calculation shows that the ground state of  $\text{TlFe}_{1.5}\text{Se}_2$  with Fe-vacancy ordered orthorhombic superstructure is an SDW phase which opens a gap only if a moderately strong electron correlation is imposed. The quantitative change of the bandwidth of Fe-3d electrons density of states (DOS) near the Fermi energy further supports the Mott localization driven by kinetic energy reduction due to Fe-vacancies. This scenario is quite similar to the Mott localization proposed for iron oxychalcogenides  $\text{La}_2\text{O}_2\text{Fe}_2\text{O}(\text{Se,S})_2$ [23], where the reduction of kinetic energy or the band narrowing is due to the expanded interatomic Fe-Fe distance. As a consequence, we predict that the Mott delocalization could also take place in  $\text{TlFe}_{2-x}\text{Se}_2$  under pressure up to  $\sim 6$  GPa.

The electronic structure calculations were performed with the Vienna Ab-initio Simulation Package (VASP)[24, 25]. All structures were optimized so that the forces on individual atoms were smaller than  $0.02$  eV/Å and the pressure convergence criterion is chosen to be 0.5 kbar. For the optimization and ground state calculations, a  $4 \times 2 \times 2$  Monkhorst-Pack k-grid[26] was employed, while  $16 \times 8 \times 8$  Monkhorst-Pack k-grid was used for the density of states (DOS) calculations. The PBE flavor of general gradient approximation (GGA) to the exchange-correlation functional[27] was applied throughout the calculations.

We first discuss the possible crystal structure and spin configurations of  $\text{TlFe}_{2-x}\text{Se}_2$  ( $x = 0.5$ ). The Mössbauer experiment suggests a body-centered orthorhombic (BCO) crystal structure of  $\text{TlFe}_{2-x}\text{Se}_2$ [28], where the Fe sheets form superstructure due to Fe-deficiency (FIG. 1). There are four possible stacking configurations for the two neighbouring Fe-layers[32], as shown in FIG. 1. We consider the AFM and

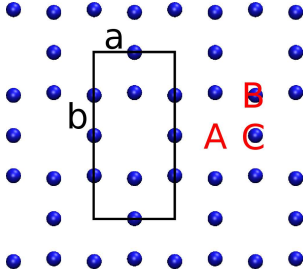


FIG. 1: Superstructure of  $\text{TlFe}_{1.5}\text{Se}_2$ .  $A$ ,  $B$ , and  $C$  correspond to three different sites directly above the Fe-vacancy, the 3-coordinated Fe site, and the 2-coordinated site, respectively. Another stacking pattern  $A'$  is that the upper-layer is rotated  $90^\circ$  around  $c$ -axis.

SDW configurations within each layers, while the interlayer coupling along  $c$ -axis can be either ferromagnetic (FM) or AFM. The relative energies (in unit of meV) for different stacking and ordering patterns are listed in Table I. We find that the ground state of  $\text{TlFe}_{2-x}\text{Se}_2$  should be of essentially two-dimensional SDW, as the energy differences among the different inter-layer magnetic orderings are very small ( $< 1\text{meV/Fe}$ ), indicating the negligible inter-layer magnetic coupling. Hence, without losing generality, we shall focus on the  $AA$ -stacking pattern in the following discussions.

We also notice that for the NM state, the full structural optimization leads to the well-known  $c$ -collapse problem; while for the SDW state, the resulting structure ( $c$  and  $z_{\text{Se}}$ ) is within the expectation. Thus, unless otherwise specified, the electronic structure calculations in the following discussions were performed with the geometry relaxed in the SDW configuration. The calculated local magnetic moment of Fe atom is then  $m_{\text{Fe}} \approx 2.6 \sim 2.7 \mu_B$ .

TABLE I: Configuration energies of  $\text{TlFe}_{1.5}\text{Se}_2$ .  $AA$ ,  $AB$ ,  $AC$  and  $AA'$  indicates the stacking geometry, while NM, AFM, SDW indicate the intralayer magnetic configurations. The superscripts  $a$  and  $f$  indicate interlayer AFM and FM orderings, respectively.

	$AA$	$AB$	$AC$	$AA'$
NM	0.0	21.4	12.7	24.
AFM <sup>f</sup>	-175	-170	-167	
AFM <sup>a</sup>	-175	-164	-166	
SDW <sup>f</sup>	-257	-259	<b>-261</b>	
SDW <sup>a</sup>	-257	-259	<b>-261</b>	

We now examine the DOS and the projected DOS (PDOS) of the  $AA$ -stacking SDW<sup>a</sup> ( Fig. 2(a) ). We find that the band gap  $E_g$  in the  $AA$ -stacking SDW<sup>a</sup> is vanishingly small for the fully optimized system under the GGA method, while other NM states are metallic. The observation is the same for other AB or AC interlayer stacking patterns. The SDW band gap is too small to compare with the activation gap  $E_a \sim 57.7$  meV observed in the  $x = 0.5$  sample [17]. It suggests that the experimentally observed gap in  $\text{TlFe}_{2-x}\text{Se}_2$  ( at least for  $x = 0.5$  ) is not due to the SDW ordering itself, but due to the Mott localization driven by the moderately strong electron

TABLE II: Geometry and magnetic properties of  $\text{TlFe}_{1.5}\text{Se}_2$ . Only the ground state (SDW) configurations are listed.  $z_{\text{Se}}$  is the internal coordinate for Se and  $m_{\text{Fe}}$  is the local magnetic moment on Fe atoms. The numbers outside and inside the brackets for  $m_{\text{Fe}}$  are for 3-coordinated and 2-coordinated Fe atoms, respectively.

		$AA$	$AB$	$AC$
SDW <sup>f</sup>	a	5.5390	5.5441	5.5441
	b	11.0189	11.0488	11.0289
	c	13.8451	13.7776	13.8349
	$z_{\text{Se}}$	0.351	0.351(0.350)	0.351
	$m_{\text{Fe}}(\mu_B)$	2.61(2.73)	2.61(2.75)	2.61(2.75)
SDW <sup>a</sup>	a	5.5507	5.5468	5.5505
	b	11.0342	11.0414	11.0256
	c	13.8027	13.7840	13.8472
	$z_{\text{Se}}$	0.351	0.351(0.350)	0.350
	$m_{\text{Fe}}(\mu_B)$	2.62(2.74)	2.62(2.74)	2.57(2.71)

correlation.

To investigate the Mott-insulating state, we extended our calculations by using the GGA+ $U$  method for  $U=0,1,2,3,4,5$  eV. The Hubbard on-site energy  $U$ -dependent band gap  $E_g$  is obtained in TAB. III. The calculated DOS for  $U = 0$  eV and  $U = 4.0$  eV is compared in FIG. 2(a). Within GGA+ $U$ , an insulating gap develops immediately with increasing  $U$ , and the projected density of states associated with Fe-3d electrons move to higher energies mainly distributed around 1 eV above the Fermi energy ( for  $U=4$  eV ).

TABLE III:  $U$ -dependency of  $E_g$

$U$ (eV)	0	1.0	2.0	3.0	4.0	5.0
$E_g$ (meV)	$< 5$	40	60	80	140	230

We have also performed calculations for  $x = 0$  and  $x = 0.4$ , respectively, keeping the Fe-vacancy ordered tetragonal superstructure in the latter case [17, 28]. For  $x = 0$  the AFM state becomes more stable than the SDW state ( in agreement with Ref.[18] ), while the overall band structure of  $\text{TlFe}_2\text{As}_2$  is similar to that of  $\text{KFe}_2\text{Se}_2$  [20]. For illustration, the band structures for  $x = 0.5$  and  $x = 0.0$  are fitted to a tight-binding model Hamiltonian by using the maximally localized wannier function (MLWF)[29, 30] method. The results are plotted in Fig. 4, where the color indicates the percentage of  $d_{zx(y)}$  and  $d_{y^2-x^2}$  composition, from 0% (blue) to 100% (red). For the  $x = 0$  structure, the Hamiltonian is particularly simple with 5-bands. The nearest neighbor hopping parameters and the on-site energies are listed in TAB. V. The bands near  $E_F$  for  $\text{TlFe}_2\text{Se}_2$  are dominated by  $d_{zx(y)}$  and  $d_{y^2-x^2}$  orbitals except for one empty band around X. For the  $x = 0.5$  structure, the Hamiltonian is too complicated due to the structural distortion, and all 5 d-orbitals are entangled considerably around  $E_F$ . Nevertheless, the Fermi surface of  $\text{TlFe}_{1.5}\text{Se}_2$  can be reconstructed from this Hamiltonian, as shown in Fig. 3.

The apparent different band structures for  $x = 0$  and

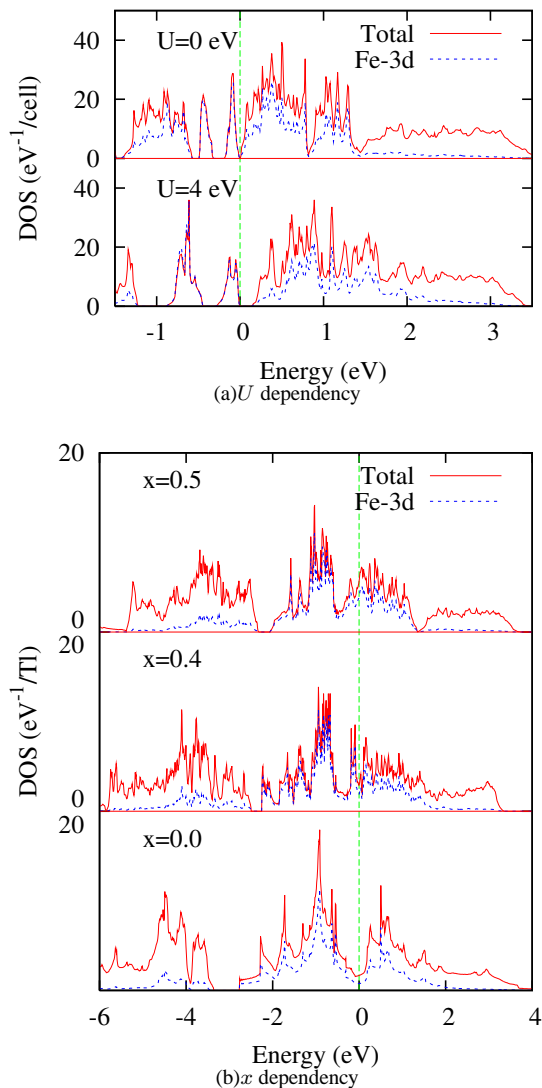


FIG. 2: Total and projected density of states of  $\text{TlFe}_{2-x}\text{Se}_2$ . 2(a) shows the  $U$  dependency of DOS at the SDW state, with  $U = 0$  eV in upper panel and  $U = 4$  eV in the lower panel; and 2(b) shows the dependence on the Fe deficiency, with  $x = 0.5$ ,  $x = 0.4$ ,  $x = 0.0$  from top to bottom panels, respectively. In all figures, the red solid lines are the total density of states, and the blue dashed lines are the DOS projected onto Fe-3d orbitals. In 2(b), all DOS are renormalized to per  $\text{TlFe}_{2-x}\text{Se}_2$  formula.

$x = 0.5$  provides an indication for the transition at certain  $0 < x_c < 0.5$ , i.e., when  $x > x_c$ , the Mott localization takes place. As the Fe-Fe distance increases less than 1% from  $x = 0$  to  $x = 0.5$  [17], this amount of lattice expansion is not sufficient for the Mott localization in  $\text{TlFe}_{2-x}\text{Se}_2$ , as compared to iron oxychalcogenides  $\text{La}_2\text{O}_2\text{Fe}_2\text{O}(\text{Se},\text{S})_2$ [23]. Here, we argue that the kinetic energy reduction caused by the Fe-vacancies should play an crucial role in driving the system to the insulating phase. An intuitive estimate is that the coordinate number of Fe in the  $\text{TlFe}_{1.5}\text{Se}_2$  is reduced to 3 or 2 depending on the Fe site comparing to 4 in a perfect square

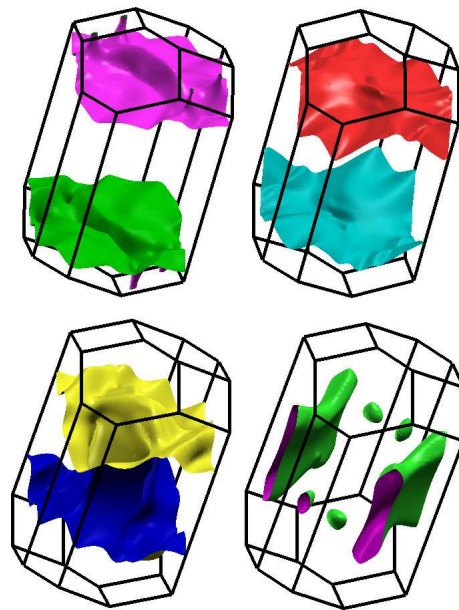


FIG. 3: Fermi surfaces of  $\text{TlFe}_{1.5}\text{Se}_2$  reconstructed using the MLWFs shown in the  $\Gamma$ -centered reciprocal BCO lattice. The fermi surface consists of four extended sheets.

lattice. Thus the total kinetic energy is substantially reduced by the Fe-vacancies, enhancing the normalized electron correlation  $U/t$ , with  $t$  being the bandwidth proportional to the kinetic energy.

Our argument can be checked by fitting band structures of  $x = 0, 0.4$  and  $0.5$  to tight-binding models. We only need to consider the NM state ( and  $U = 0$  ) and calculate the hopping terms summed around a specific Fe atom,  $T_i = \sum_{i+\delta} t_{i,i+\delta}$ . Using the fitted Hamiltonian we obtain  $T_i = 7.79$  and  $4.99$  eV for  $x = 0$  and  $0.4$ , respectively. While for  $x = 0.5$ , we obtain  $T_i = 5.67$  or  $3.44$  eV, corresponding to 3- or 2-coordinated Fe-sites, respectively. As the ratio of their numbers is 2:1, the average kinetic energy is  $4.93$  eV. The simple energetic consideration indicates that the ground states for  $x = 0.4$  and  $x = 0.5$  is very close to each other. For comparison, the DOS's ( setting  $U = 0$  for the NM state ) for  $x = 0, 0.4$ , and  $0.5$  are plotted in Fig. 2(b). The Fe-3d bandwidths are roughly  $4.8$  eV,  $3.8$  eV, and  $3.5$  eV, respectively. Thus, we indeed find a substantial enhancement of the normalized electron correlation, manifesting the kinetic energy reduction caused by Fe-vacancies.

TABLE IV: Pressure dependency of crystal structure and band gap width.

$P$ (GPa)	0	2	4	6
$a$ ( $\text{\AA}$ )	5.5507	5.4517	5.3716	5.3079
$b$ ( $\text{\AA}$ )	11.0342	10.8842	10.7283	10.6177
$c$ ( $\text{\AA}$ )	13.8027	13.5166	13.2874	13.1102
$E_{\text{cell}}$ (eV)	-187.01	-186.65	-185.91	-158.00
$E_g$ (meV)	140	80	50	0

Finally, an alternative route to the Mott (de-)localization is to apply the physical pressure, which can lead to bandwidth expansion by lattice contraction. The numerical results for the pressure dependent band gap  $E_g$  with fixed  $U = 4.0$  eV are listed in TAB. IV ( $x = 0.5$ ). From these results we expect that the activation gap, which is about 60 meV or well below 150 meV [17], can be completely suppressed by applying pressure up to 6 GPa.

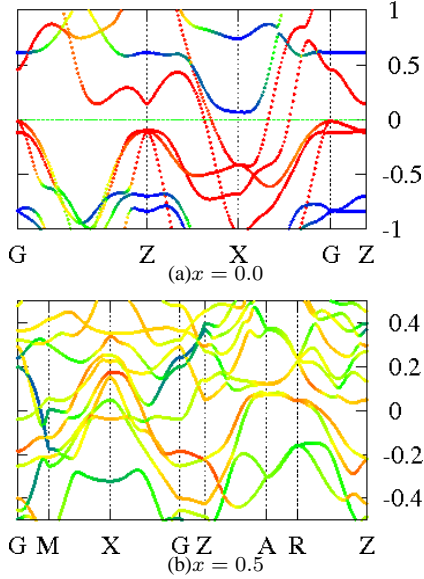


FIG. 4: Band structures of  $\text{TlFe}_{2-x}\text{Se}_2$  with 4(a)  $x = 0.0$  and 4(b)  $x = 0.5$  fitted using MLWF.

TABLE V: Tight-binding Hamiltonian terms for  $\text{TlFe}_{2-x}\text{Se}_2$  ( $x = 0.0$ ). Only the nearest neighbor hoppings and on-site energies are shown here. The numbers along the diagonal line inside the brackets are the on-site terms, while the others are the hoppings. All numbers are in eV.

	$d_{z^2}$	$d_{zx}$	$d_{zy}$	$d_{x^2-y^2}$	$d_{xy}$
$d_{z^2}$	-0.019 (4.765)	0	0.156	0.303	0
$d_{zx}$	0	-0.028 (5.084)	0	0	0.286
$d_{zy}$	0.156	0	-0.314 (5.084)	-0.344	0
$d_{x^2-y^2}$	-0.303	0	-0.344	-0.378 (4.600)	0.0
$d_{xy}$	0	0.286	0	0	-0.047 (5.056)

To summarize, we find that for  $\text{TlFe}_{1.5}\text{Se}_2$ , the electronic band structure shows a band gap only when the short-ranged Coulomb interaction  $U$  beyond LDA/GGA is considered. From the experimentally observed activation gap,  $U$  should be at least 2eV. The corresponding ground state is then a stripe-like anti-ferromagnetic Mott insulator, which persists at least

to  $\text{TlFe}_{1.6}\text{Se}_2$  with Fe-vacancy-ordered tetragonal superstructure, and the superstructure of various Fe-vacancy ordering patterns is important for the stability of the Mott insulating phase. We predict that the activation gap in  $\text{TlFe}_{1.5}\text{Se}_2$  can be completely suppressed under pressure up to  $\sim 6$  GPa and the SC may emerge.

We would like to express special thanks to M. Fang and Q. Si for helpful discussions. We are also grateful for the discussions with G. Cao, H. Wang, Z. Xu, and H. Yuan. This work was supported by the NSFC, the 973 Project of the MOST and the Fundamental Research Funds for the Central Universities of China (No. 2010QNA3026). All the calculations were performed at High Performance Computing Center of Hangzhou Normal University.

Note added: After completing this work, we became aware of two recent papers by X.W. Yan et al.[31], where independent first-principle calculations on electronic structure and magnetic properties are reported for the cases of  $x = 0$  and  $x = 0.5$ .

- 
- [1] Y. Kamihara, T. Watanabe, M. Hirano, and H. Hosono, *J. Am. Chem. Soc.* **130**, 3296 (2008).
  - [2] X. H. Chen, G. W. T. Wu, R. H. Liu, H. Chen, and D. F. Fang, *Nature* **453**, 761 (2008).
  - [3] G. F. Chen, Z. Li, D. Wu, G. Li, W. Z. Hu, J. Dong, P. Zheng, J. L. Luo, and N. L. Wang, *Phys. Rev. Lett.* **100**, 247002 (2008).
  - [4] Z. Ren, G. Che, X. Dong, J. Yang, W. Lu, W. Yi, X. Shen, Z. Li, L. Sun, F. Zhou, et al., *Europhys. Lett.* **83**, 17002 (2008).
  - [5] H. H. Wen, G. Mu, L. Fang, H. Yang, and X. Zhu, *Europhys. Lett.* **82**, 17009 (2008).
  - [6] C. Wang, L. Li, S. Chi, Z. Zhu, Z. Ren, Y. Li, Y. Wang, X. Lin, Y. Luo, X. Xu, et al., *Europhys. Lett.* **83**, 67006 (2008).
  - [7] M. M. Q. *et al.*, *Nature Phys.* **5**, 647 (2009).
  - [8] C. de la Cruz *et al.*, *Nature* (453).
  - [9] J. D. *et al.*, *Europhys. Lett.* **83**, 270069 (2008).
  - [10] D. J. Singh and M. H. Du, *Phys. Rev. Lett.* **100**, 237003 (2008).
  - [11] I. I. Mazin, D. J. Singh, M. D. Johannes, and M. H. Du, *Phys. Rev. Lett.* **101**, 057003 (2008).
  - [12] T. Yildirim, *Phys. Rev. Lett.* **101**, 057010 (2008).
  - [13] Q. Si and E. Abrahams, *Phys. Rev. Lett.* **101**, 076401 (2008).
  - [14] C. Cao, P. J. Hirschfeld, and H.-P. Cheng, *Phys. Rev. B* **77**, 220506 (2008).
  - [15] F. Ma and Z. Y. Lu, *Phys. Rev. B* **78**, 033111 (2008).
  - [16] F. Ma, Z. Y. Lu, and T. Xiang, *Phys. Rev. B* **78**, 2245179 (2008).
  - [17] M. Fang, H. Wang, C. Dong, Z. Li, Li, C. Feng, J. Chen, and H. Yuan (2010), arXiv:1012.5236.
  - [18] L. Zhang and D. J. Singh, *Phys. Rev. B* **79**, 094528 (2009).
  - [19] I. Shein and A. Ivanovskii (2010), arXiv:1012.5164.
  - [20] C. Cao and J. Dai (2010), arXiv:1012.5621.
  - [21] J. Guo, S. Jin, G. Wang, K. Zhu, M. He, and X. L. Chen, *Phys. Rev. B* **82**, 180520(R) (2010).
  - [22] A. K.-M. *et al.* (2010), arXiv:1012.3637.
  - [23] J. X. Zhu, R. Yu, H. Wang, L. L. Zhao, M. D. Jones, J. Dai, E. Abrahams, E. Morosan, M. H. Fang, and Q. Si, *Phys. Rev. Lett.* **104**, 216405 (2010).
  - [24] G. Kresse and J. Hafner, *Phys. Rev. B* **47**, 558 (1993).
  - [25] G. Kresse and D. Joubert, *Phys. Rev. B* **59**, 1758 (1999).
  - [26] H. J. Monkhorst and J. D. Pack, *Phys. Rev. B* **13**, 5188 (1976).

- [27] J. Perdew, K. Burke, and M. Ernzerhof, Phys. Rev. Lett. **77**, 3865 (1996).
- [28] L. Haggstrom and A. Seidel, J.Mag.Mag. Mat. **98**, 37 (1991).
- [29] I. Souza, N. Marzari, and D. Vanderbilt, Phys. Rev. B **65**, 035109 (2001).
- [30] A. A. Mostofi, J. R. Yates, Y.-S. Lee, I. Souza, D. Vanderbilt, and N. Marzari, Comp. Phys. Comm. (2007), arXiv:0708.0650.
- [31] X. W. Yan, M. Gao, Z. Y. Lu, and T. Xiang (2010), arXiv:1012.5536v1; arXiv:1012.6015v1.
- [32] We find that the Fe-deficiency will induce structural relaxation in general, which leads to the distortion of the square Fe lattice and the small displacement of Fe atoms. Thus the  $AA'$ -stacking is energetically unfavorable and is not considered here.